

## LETTER TO THE EDITOR

## Unique Fermi surfaces with quasi-one-dimensional character in $\text{CeRh}_3\text{B}_2$ and $\text{LaRh}_3\text{B}_2$

T Okubo<sup>1</sup>, M Yamada<sup>1</sup>, A Thamizhavel<sup>1</sup>, S Kirita<sup>1</sup>, Y Inada<sup>1,5</sup>, R Settai<sup>1</sup>, H Harima<sup>2</sup>, K Takegahara<sup>3</sup>, A Galatanu<sup>4</sup>, E Yamamoto<sup>4</sup> and Y Ōnuki<sup>1,4</sup>

<sup>1</sup> Graduate School of Science, Osaka University, Toyonaka, Osaka 560-0043, Japan

<sup>2</sup> The Institute of Scientific and Industrial Research, Osaka University, Ibaraki, Osaka 567-0047, Japan

<sup>3</sup> Department of Materials Science and Technology, Hirosaki University, Hirosaki, Aomori 036-8561, Japan

<sup>4</sup> Advance Science Research Centre, Japan Atomic Energy Research Institute, Tokai, Ibaraki 319-1195, Japan

Received 13 October 2003

Published 7 November 2003

Online at [stacks.iop.org/JPhysCM/15/L721](http://stacks.iop.org/JPhysCM/15/L721)

### Abstract

We have carried out de Haas–van Alphen (dHvA) experiments on a ferromagnet  $\text{CeRh}_3\text{B}_2$  with an extremely high Curie temperature  $T_C \simeq 120$  K and a non-4f reference compound  $\text{LaRh}_3\text{B}_2$ . The dHvA data of  $\text{LaRh}_3\text{B}_2$  are well explained by the results of energy band calculations. The topology of the Fermi surfaces in  $\text{CeRh}_3\text{B}_2$  is found to be very similar to that of  $\text{LaRh}_3\text{B}_2$ , possessing wavy but flat Fermi surfaces in the basal plane. Observation of a quasi-one-dimensional electronic state is the first such case in a rare earth compound.

In order to gain a deeper understanding of magnetic and superconducting properties in cerium and uranium compounds, it is essentially important to clarify the nature of the f electrons: namely whether they are itinerant or localized. This issue is closely related to the strongly correlated nature of conduction electrons, which hinders the conduction electrons to move freely due to the strong Coulomb repulsion, and consequently these electrons have tendency to localize. The strongly correlated electrons are thus found to behave in some cases like itinerant electrons and in other cases like localized electrons, depending on the temperature region and/or on the compound [1, 2].

$\text{CeRh}_3\text{B}_2$ , with the hexagonal structure of space group  $P6/mmm$  (#191), has attracted a considerable interest due to its anomalous ferromagnetic properties [3–5]. The Curie temperature  $T_C \simeq 120$  K is the highest value in the cerium compounds. Surprisingly the Curie temperature  $T_C \simeq 120$  K is far above  $T_C = 91$  K in  $\text{GdRh}_3\text{B}_2$ . This means that  $T_C \simeq 120$  K in

<sup>5</sup> On leave from: Osaka University, Faculty of Education, Okayama University, 3-1-1 Tsushimanaka, Okayama 700-8530, Japan.

$\text{CeRh}_3\text{B}_2$  is two orders of magnitude higher than the magnetic ordering temperature expected from the de Gennes factor consideration. An ordered magnetic moment of  $0.4 \mu_{\text{B}}/\text{Ce}$ , which is oriented within the basal plane, is relatively small compared to the usual value of about  $1 \mu_{\text{B}}/\text{Ce}$  [6].

The hexagonal crystal structure is anomalous. The  $c$ -value of  $3.096 \text{ \AA}$  at room temperature is very short, smaller than  $3.41 \text{ \AA}$  in  $\alpha$ -Ce with valence close to  $4+$ , namely without  $4f$  magnetism, while the  $a$ -value of  $5.469 \text{ \AA}$  is normal [7–9]. The temperature dependence of the lattice constants for  $\text{LaRh}_3\text{B}_2$ ,  $\text{CeRh}_3\text{B}_2$  and a ferromagnet  $\text{PrRh}_3\text{B}_2$  with  $T_{\text{C}} = 2 \text{ K}$  indicates that both the  $a$ - and  $c$ -values of  $\text{LaRh}_3\text{B}_2$  and  $\text{PrRh}_3\text{B}_2$  monotonously decrease with decreasing temperature, while in  $\text{CeRh}_3\text{B}_2$  the  $a$ -value increases below  $300 \text{ K}$  and consequently the  $c$ -value decreases steeply below  $300 \text{ K}$ . The quasi-one-dimensional character along the  $c$ -axis is enhanced at lower temperatures in  $\text{CeRh}_3\text{B}_2$ .

From these experimental results it was suggested that ferromagnetism is not based on the  $4f$  localized moment but an intermediate valence or even itinerant magnetism [3, 4, 9]. On the other hand, NMR, photoemission spectroscopy, x-ray absorption spectroscopy experiments as well as a La-substitution study indicated that there are no magnetic moments on the Rh and B sites and the magnetic moment is located on the Ce atom [10–13]. From a polarized neutron scattering study, it was clarified that the magnetic moment of the cerium ion is  $\mu_{\text{Ce}} = \mu_{4f} + \mu_{5d} = 0.38 \mu_{\text{B}}$ : the  $4f$  magnetic moment  $\mu_{4f} = +0.56 \mu_{\text{B}}$  and the non-negligible Ce  $5d$  magnetic moment  $\mu_{5d} = -0.18 \mu_{\text{B}}$  [14]. This value is in good agreement with the experimental value of  $0.4 \mu_{\text{B}}$ . Quite recently the ferromagnetism in  $\text{CeRh}_3\text{B}_2$  has been theoretically discussed on the basis of a two-band model of which the basic ingredient is an uncorrelated dispersive band hybridized with a correlated and narrow band [15].

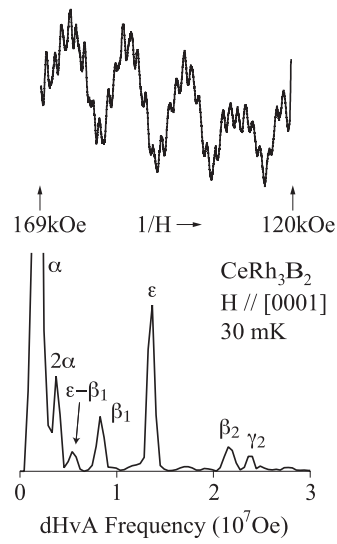
This letter reports the first experimental results of de Haas–van Alphen (dHvA) oscillations to clarify the Fermi surface property. These experiments on  $\text{CeRh}_3\text{B}_2$  were not carried out previously mainly due to the poor quality of the single crystal sample. The experimental results on  $\text{CeRh}_3\text{B}_2$  are compared to the dHvA results of a corresponding non- $4f$  reference compound  $\text{LaRh}_3\text{B}_2$  and the theoretical results of full potential LAPW (FLAPW) band calculations of  $\text{LaRh}_3\text{B}_2$ , indicating the existence of unique Fermi surfaces, namely wavy but flat Fermi surfaces in the basal plane.

Single crystals of  $\text{CeRh}_3\text{B}_2$  and  $\text{LaRh}_3\text{B}_2$  were grown by the Czochralski pulling method in a tetra-arc furnace. Starting materials were 99.9%-pure Ce and La, 99.99%-pure Rh and 99.99%-pure B. Ingots were about  $3 \text{ mm}$  in diameter and  $40 \text{ mm}$  in length, which were annealed at  $900 \text{ }^\circ\text{C}$  in high vacuum of  $10^{-10} \text{ Torr}$ .

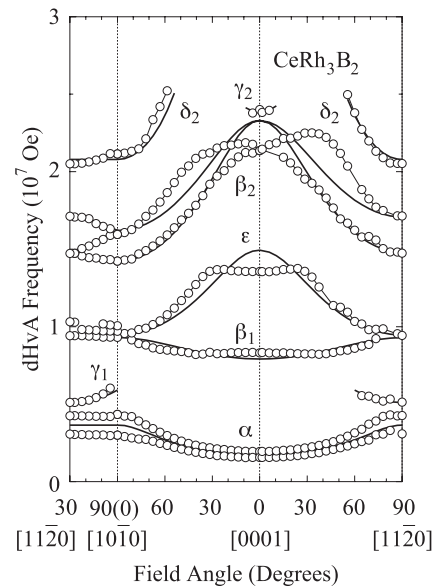
The residual resistivity  $\rho_0$  and residual resistivity ratio  $\rho_{\text{RT}}/\rho_0$  in  $\text{CeRh}_3\text{B}_2$  were  $\rho_0 = 2.0 \mu\Omega \text{ cm}$  and  $\rho_{\text{RT}}/\rho_0 = 58$  for the current along  $[10\bar{1}0]$ . This indicates the best quality sample, as far as we know. The corresponding values of  $\text{LaRh}_3\text{B}_2$  were  $\rho_0 = 1.1 \mu\Omega \text{ cm}$  and  $\rho_{\text{RT}}/\rho_0 = 89$ . The dHvA experiments were done at high magnetic fields up to  $170 \text{ kOe}$  and low temperatures down to  $30 \text{ mK}$ . The dHvA voltage was obtained in the so-called  $2\omega$  detection of the field modulation method [1].

Figure 1 shows the typical dHvA oscillation in the field range from  $120$  to  $169 \text{ kOe}$  at  $30 \text{ mK}$  for  $H \parallel [0001]$  ( $c$ -axis) and the corresponding fast Fourier transformation (FFT) spectrum of  $\text{CeRh}_3\text{B}_2$ . We detected five kinds of fundamental branches, named  $\alpha$ ,  $\beta_1$ ,  $\varepsilon$ ,  $\beta_2$  and  $\gamma_2$ , together with harmonics, where the dHvA frequency  $F(=c\hbar/2\pi e)S_{\text{F}}$  is proportional to an extremal (maximum or minimum) cross-sectional area  $S_{\text{F}}$  of the Fermi surface. From the temperature dependence of the dHvA amplitude, we can determine the cyclotron effective mass  $m_{\text{c}}^*$ . The cyclotron mass is rather light, ranging from  $0.3$  to  $3 m_0$ .

Figure 2 shows the angular dependence of the dHvA frequency. Each branch is characterized as follows.



**Figure 1.** dHvA oscillation and its FFT spectrum for the field along [0001] in  $\text{CeRh}_3\text{B}_2$ .



**Figure 2.** Angular dependence of the dHvA frequency in  $\text{CeRh}_3\text{B}_2$ . Thick solid curves correspond to the Fermi surfaces shown in figures 4(f)–(j).

- (1) branch  $\alpha$ : an ellipsoidal Fermi surface elongated along [0001], which is most likely split into two kinds of Fermi surfaces with up- and down-spin states;
- (2) branch  $\beta_1$ : an approximately spherical Fermi surface;
- (3) branch  $\epsilon$ : an ellipsoidal Fermi surface shrunken along [0001];
- (4) branch  $\beta_2$ : three ellipsoidal Fermi surfaces;
- (5) branch  $\delta_2$ : a flat ellipsoidal Fermi surface.

The other branches,  $\gamma_1$  and  $\gamma_2$ , are detected in the basal plane and around [0001], respectively.

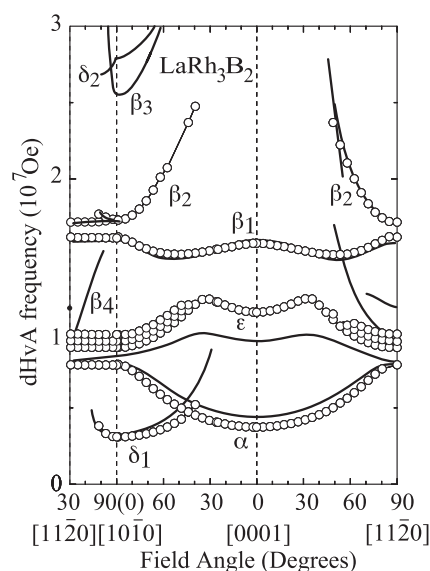


**Figure 3.** Angular dependence of the dHvA frequency in  $\text{LaRh}_3\text{B}_2$ . Thick solid curves correspond to the theoretical Fermi surfaces.

We can estimate the topology of the corresponding Fermi surface, which is shown by thick solid curves in figure 2. The exact Fermi surface is discussed later on the basis of the Fermi surface of  $\text{LaRh}_3\text{B}_2$ .

To understand the topology of the Fermi surface in  $\text{CeRh}_3\text{B}_2$ , we have also carried out the same dHvA experiments for  $\text{LaRh}_3\text{B}_2$ . We show in figure 3 the angular dependence of the dHvA frequency of  $\text{LaRh}_3\text{B}_2$ . Branches  $\alpha$ ,  $\beta_1$  and  $\varepsilon$  in  $\text{LaRh}_3\text{B}_2$  are very similar to the corresponding branches in  $\text{CeRh}_3\text{B}_2$ , although the absolute magnitude of the dHvA frequency is slightly different. The cyclotron mass of  $\text{LaRh}_3\text{B}_2$  is in the range from 0.3 to 1.3  $m_0$ .

The solid curves in figure 3 indicate the theoretical results based on the FLAPW band calculations, which are in good agreement with the experimental results. The calculations were performed by modifying the local density approximation (LDA) for the exchange–correlation potential. We found that the slight modification of the LDA band structure is necessary to describe the experimental Fermi surfaces. The La 4f and La 5d levels were artificially shifted upward from the LDA levels by 0.2 and 0.1 Ryd, respectively. Such modifications were important to construct the previous Fermi surface study in  $\text{LaB}_6$  [16] and  $\text{YbAl}_3$  [17], for example. The lattice constants used for the calculations were  $a = 5.480 \text{ \AA}$  and  $c = 3.137 \text{ \AA}$  [7]. The density of states at the Fermi level is calculated as  $7.37 \text{ mJ K}^{-2} \text{ mol}^{-1}$ . The results of the band structure calculations, together with the method, will be published in a separated paper [18].

The theoretical Fermi surfaces are shown in figures 4(a)–(e), where bands 30 and 31 correspond to hole Fermi surfaces and bands 32–34 are due to compensated electron Fermi surfaces, indicating that  $\text{LaRh}_3\text{B}_2$  is a compensated metal with equal volumes of electron and hole Fermi surfaces. It is noted that there exist two kinds of quasi-one-dimensional flat bands 32- and 33-electron Fermi surfaces. The dHvA branches named  $\alpha$ ,  $\beta_i$ ,  $\delta_i$  and  $\varepsilon$  are identified in the Fermi surfaces in figures 4(a)–(e). Theoretical orbits named  $\beta_3$ ,  $\beta_4$  and  $\delta_2$  are, however, not detected experimentally most likely because of a small curvature factor of these orbits. Moreover, a quasi-one-dimensional band 32-electron Fermi surface cannot be detected in the dHvA experiment because of no closed orbits.

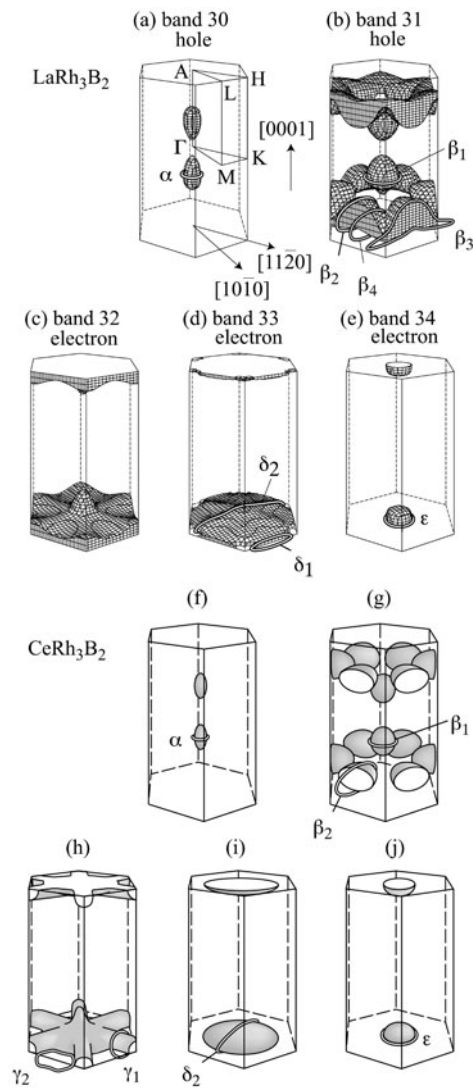


**Figure 4.** (a)–(e) Theoretical Fermi surfaces in  $\text{LaRh}_3\text{B}_2$ , and (f)–(j) Fermi surfaces obtained experimentally in  $\text{CeRh}_3\text{B}_2$ .

On the basis of these Fermi surfaces in  $\text{LaRh}_3\text{B}_2$ , we simply constructed the corresponding Fermi surfaces for  $\text{CeRh}_3\text{B}_2$ , which are shown in figures 4(f)–(j), together with the thick solid curves in figure 2. Our analyses are as follows. Branches  $\alpha$ ,  $\beta_1$  and  $\epsilon$  are in principle unchanged between  $\text{LaRh}_3\text{B}_2$  and  $\text{CeRh}_3\text{B}_2$ , although the volume of the each Fermi surface is slightly changed. The connected band 31-hole Fermi surfaces named  $\beta_2$ ,  $\beta_3$  and  $\beta_4$  of  $\text{LaRh}_3\text{B}_2$  in figure 4(b) are separated into three ellipsoidal Fermi surfaces in  $\text{CeRh}_3\text{B}_2$ . The flat quasi-one-dimensional band 33-electron Fermi surface of  $\text{LaRh}_3\text{B}_2$  is changed into a flat ellipsoidal closed Fermi surface in  $\text{CeRh}_3\text{B}_2$ . The quasi-one-dimensional band 32-electron Fermi surface of  $\text{LaRh}_3\text{B}_2$  is also changed into a multiply connected Fermi surface with arms named  $\gamma_1$  along  $[11\bar{2}0]$ . The volume of hole Fermi surfaces in  $\text{CeRh}_3\text{B}_2$  is as follows:  $0.002 V_{\text{BZ}}$  for branch  $\alpha$ ,  $0.012 V_{\text{BZ}}$  for two branches  $\beta_1$  and  $0.105 V_{\text{BZ}}$  for these branches  $\beta_2$ , indicating a total volume

of  $0.12 V_{\text{BZ}}$  for the hole Fermi surfaces, where  $V_{\text{BZ}}$  is the volume of the Brillouin zone. The corresponding compensated electron Fermi surfaces are  $0.008 V_{\text{BZ}}$  for branch  $\varepsilon$  and  $0.039 V_{\text{BZ}}$  for branch  $\delta_2$ . A remaining volume of  $0.07 V_{\text{BZ}}$  is expected for the band 32-electron Fermi surface and is shown in figure 4(h).  $\text{CeRh}_3\text{B}_2$  is also a compensated metal.

The present analysis is in principle based on the 4f localized model. The contribution of the 4f localized electron to the volume of the Fermi surface is thus small. Even in the localized system, however, the presence of the 4f electron alters the Fermi surface through the 4f electron contribution to the crystal potential and through the introduction of magnetic Brillouin zone boundaries and magnetic energy gaps which occur when the 4f electron moments order. We note that the Fermi surfaces with up- and down-spin states are not observed, apart from a small Fermi surface named  $\alpha$ . This is mainly due to a small ordered moment of  $0.4 \mu_{\text{B}}/\text{Ce}$ .

The electronic specific heat coefficient in  $\text{CeRh}_3\text{B}_2$  is approximately estimated from the cyclotron mass:  $0.27 \text{ mJ K}^{-2} \text{ mol}^{-1}$  for branch  $\alpha$  ( $m_{\text{c}}^* = 0.33 m_0$  and  $0.37 m_0$  for  $H \parallel [0001]$ ),  $0.55 \text{ mJ K}^{-2} \text{ mol}^{-1}$  for two branches  $\beta_1$  ( $m_{\text{c}}^* = 0.60 m_0$  for  $H \parallel [0001]$ ),  $8.67 \text{ mJ K}^{-2} \text{ mol}^{-1}$  for three branches  $\beta_2$  ( $m_{\text{c}}^* = 2.0 m_0$  for  $H \parallel [0001]$  and  $1.9 m_0$  for  $H \parallel [10\bar{1}0]$ ),  $2.7 \text{ mJ K}^{-2} \text{ mol}^{-1}$  for branch  $\delta_2$  ( $m_{\text{c}}^* = 2.4 m_0$  for  $H \parallel [10\bar{1}0]$ ), and  $1.1 \text{ mJ K}^{-2} \text{ mol}^{-1}$  for branch  $\varepsilon$  ( $m_{\text{c}}^* = 2.3 m_0$  for  $H \parallel [0001]$  and  $1.7 m_0$  for  $H \parallel [10\bar{1}0]$ ), indicating a total of about  $13 \text{ mJ K}^{-2} \text{ mol}^{-1}$ . The electronic specific heat coefficient of  $\text{CeRh}_3\text{B}_2$  is reported as 16 and  $20 \text{ mJ K}^{-2} \text{ mol}^{-1}$  [5, 19], while our specific heat measurement indicated  $18 \text{ mJ K}^{-2} \text{ mol}^{-1}$ . The remaining band 32-electron Fermi surface, shown in figure 4(h), is thus expected to possess about  $5 \text{ mJ K}^{-2} \text{ mol}^{-1}$ , approximately reasonable from the volume of its Fermi surface. These results indicate that the present Fermi surfaces shown in figures 4(f)–(j) are complete and there exist no other large Fermi surfaces in  $\text{CeRh}_3\text{B}_2$ .  $\text{CeRh}_3\text{B}_2$  is thus not a heavy fermion compound. This is most likely due to an extremely high ordered temperature and the nature of almost localized 4f electrons.

Quite recently ferromagnetism was theoretically discussed on the basis of a two-band model of which the basic ingredient is an uncorrelated dispersive band (mainly Rh 4d orbitals) hybridized with a correlated and narrow 4f band [15]. It is not clear whether this theory is applied to  $\text{CeRh}_3\text{B}_2$  or not. From the present dHvA results, it is important to consider that the contribution of the 4f electron to the volume of the Fermi surface is small because the topology of the Fermi surface in  $\text{CeRh}_3\text{B}_2$  is very similar to that of  $\text{LaRh}_3\text{B}_2$ , although the total volume of the Fermi surface in  $\text{CeRh}_3\text{B}_2$  is slightly smaller than that of  $\text{LaRh}_3\text{B}_2$  and each Fermi surface is slightly different between two compounds.

The short distance of the lattice constant along  $[0001]$  is found to be reflected as wavy but flat Fermi surfaces in the basal plane, which is mainly due to a well-hybridized band of Rh 4d and B 2p electrons. Observation of these unique Fermi surfaces with a quasi-one-dimensional character is the first such case in a rare earth compound. This might be related to the origin of the high Curie temperature, together with the hybridization effect between the conduction electrons and almost localized 4f electrons.

We are grateful to Professor Y Kuramoto for helpful discussion. This work was supported by the Grant-in-Aid for COE Research (10CE2004) of the Ministry of Education, Culture, Sports, Science and Technology.

## References

- [1] Ōnuki Y, Goto T and Kasuya T 1991 *Materials Science and Technology* vol 3A, ed K H J Buschow (Weinheim: VCH) p 545
- [2] Ōnuki Y, Inada Y, Ohkuni H, Settai R, Kimura N, Aoki H, Haga Y and Yamamoto E 2000 *Physica B* **280** 276
- [3] Dhar S K, Malik S K and Vijayaraghavan R 1981 *J. Phys. C: Solid State Phys.* **14** L321

- [4] Malik S K, Vijayaraghavan R, Wallace W E and Dhar S K 1983 *J. Magn. Magn. Mater.* **37** 303
- [5] Yang K N, Torikachvili M S, Maple M B and Ku H C 1984 *J. Low Temp. Phys.* **56** 601
- [6] Kasaya M, Okabe A, Takahashi T, Satoh T and Kasuya T 1988 *J. Magn. Magn. Mater.* **76/77** 347
- [7] Ku H C, Meisner G P, Acker F and Johnston D C 1980 *Solid State Commun.* **35** 91
- [8] Langen J, Jackel G, Schlabit W, Veit M and Wohlleben D 1987 *Solid State Commun.* **64** 169
- [9] Misemer D K, Auluck S, Kobayashi S I and Harmon B N 1984 *Solid State Commun.* **52** 955
- [10] Kitaoka Y, Kishimoto Y, Asayama K, Kohara T, Takeda T, Vijayaraghavan R, Malik S K, Dhar S K and Rambabu D 1985 *J. Magn. Magn. Mater.* **52** 449
- [11] Fujimori A, Takahashi T, Okabe A, Kasuya M and Kasuya T 1990 *Phys. Rev. B* **41** 6783
- [12] Schillé J Ph, Bertran F, Finazzi M, Brouder Ch, Kappler J P and Krill G 1994 *Phys. Rev. B* **50** 2985
- [13] Shaheen S A, Schilling J S and Shelton R N 1985 *Phys. Rev. B* **31** 656
- [14] Alonso J A, Boucherle J X, Givord F, Schweizer J, Gillon B and Lejay P 1998 *J. Magn. Magn. Mater.* **177–181** 1048
- [15] Batista C D, Bonča J and Gubernatis J E 2002 *Phys. Rev. Lett.* **88** 187203
- [16] Harima H, Sakai O, Kasuya T and Yanase A 1988 *Solid State Commun.* **66** 603
- [17] Ebihara T, Inada Y, Murakawa M, Uji S, Terakura C, Terashima T, Yamamoto E, Haga Y, Ōnuki Y and Harima H 2000 *J. Phys. Soc. Japan* **69** 895
- [18] Harima H and Takegahara K 2003 in preparation
- [19] Shaheen S A, Shilling J S, Klavins P, Vining C B and Shelton R N 1985 *J. Magn. Magn. Mater.* **47/48** 285